Astronomy Reports, Vol. 47, No. 6, 2003, pp. 458–466. Translated from Astronomicheskiĭ Zhurnal, Vol. 80, No. 6, 2003, pp. 499–507.

Radio and Optical Spectral Studies of Radio Sources

V. L. Afanas'ev[1], S. N. Dodonov[1], A. V. Moiseev[1], A. G. Gorshkov[2], V. K. Konnikova[2], and M. G. Mingaliev[1]

[1]*Special Astrophysical Observatory, Nizhniĭ Arkhyz, Russia*

[2]*Sternberg Astronomical Institute, Universitetskiĭ pr. 13, 119992 Moscow, Russia*

Received March 26, 2002; in final form, January 15, 2003

Abstract—Optical identifications and an analysis of the radio spectra of eight radio sources from a flux-density-complete sample at declinations 4°–6° (B1950) are presented. The observations were carried out at 4000–9000 Å on the 6-m telescope of the Special Astrophysical Observatory and at 0.97–21.7 GHz on the RATAN-600 telescope. Five of the eight sources are quasars and three are emission-line radio galaxies.

1. INTRODUCTION

This paper presents results of optical identifications of radio sources from a sample complete to a specified flux density. This work is targeted at deriving the radio luminosity function of the sample objects and its cosmological dependences. This requires that the redshifts of the majority of the sample objects be known.

All the objects whose spectra are presented here are optical counterparts of radio sources from a complete sample derived from the Zelenchuk survey at 3.9 GHz. This sample, which we have studied since 1980, contains all sources with fluxes $S_{3.9} > 200$ mJy, declinations 4°–6° (B1950), right ascensions 0–24 h, and Galactic latitudes $|b| > 10°$ [1–3]. Currently, approximately 75% of the flat-spectrum sources in the sample have been optically classified. Previous results on optical identifications of the sample objects are published in [4–6].

2. RADIO AND OPTICAL OBSERVATIONS

Optical spectra of the objects were obtained in June and November 2000 on the 6-m telescope of the Special Astrophysical Observatory (SAO) of the Russian Academy of Sciences. The observations of 1522+0400 and 1600+0412 were obtained using a multipupil spectrograph (http://www.sao.ru/gafan/devices/mpfs/mpfs_main.htm) with a TK1024 CCD detector, which has 1024 × 1024 channels and a counting noise of three electrons. The wavelength range observed was 4000–9000 Å, with a dispersion of 5 Å/pixel. The effective instrumental resolution was about 15 Å. The spectra of the remaining objects were obtained using the multipurpose SCORPIO instrument (http://www.sao.ru/moisav/scorpio/scorpio.html) in its long-slit mode together with the same CCD detector; the wavelength range was 3800–9200 Å, with a dispersion of about 6 Å/pixel. The effective instrumental resolution was about 20 Å. The spectra were reduced in the standard way using programs developed in the Laboratory of Spectroscopy and Photometry of the SAO.

Radio observations of the sample sources were carried out on the Southern sector of the RATAN-600 plane-reflector radio telescope at 3.9 and 7.5 GHz in 1980–1991 and on the Northern sector at 0.97, 2.3, 3.9, 7.7, 11.1, and 21.7 GHz in 1996–1999. The parameters of the receivers used on the Southern and Northern sectors are described in [1, 7], respectively, and the characteristics of the antenna beams for the Northern and Southern sectors are presented in [2, 8]. In each series of observations, the sources were observed daily for from 15 to 100 days.

The observations on the Northern sector of the RATAN-600 were obtained in a fixed-focus regime [9]. The position of the main mirror could be adjusted within elevations of ±1° from the center of the observation zone. An equal number of panels was used at all elevations, in order to reduce the influence of variations in the radiation of the edge panels in the presence of variations in the curvature of the circular reflector. The effective area of the antenna was taken to be constant at all elevations.

The source 2128+048 was used as a calibrator for all observations at declinations 4°–6°. The size of this radio source is much less than the horizontal section of the antenna beam at all frequencies, right up to 21.7 GHz. The flux density of 2128+048 was taken

1063-7729/03/4706-0458$24.00

Table 1. Object coordinates

Source name	Radio coordinates J2000.0		Optical–radio		Ref
	RA	DEC	ΔRA	ΔDEC	
0323+0446	03 23 14.72	+04 46 12.59	0.02^{s}	$0.01''$	JVAS
0323+0534	03 23 20.21	+05 34 11.20	0.05	1.10	NVSS
0354+0441	03 54 24.13	+04 41 07.27	−0.02	0.21	JVAS
0357+0542	03 57 46.13	+05 42 31.28	0	−0.04	JVAS
0427+0457	04 27 47.57	+04 57 08.34	0.02	−0.10	JVAS
1522+0400	15 22 32.76	+04 00 29.70	0.05	0.18	NVSS
1600+0412	16 00 02.54	+04 12 57.84	0	0.03	JVAS
2301+0609	23 01 53.46	+06 09 12.84	−0.02	0.03	JVAS

to be 4.25, 3.07, 2.35, 1.57, 1.24, and 0.75 Jy at 0.97, 2.3, 3.8, 7.7, 11.1, and 21.7 GHz, respectively.

The data were reduced using programs that enabled derivation of the flux density for an individual scan of a source, as well as determination of the mean flux density over the entire series of observations. The basis of the data reduction was optimal filtration of the input data using the method described in detail in [10]. Before this filtration, nonlinear filters were used to clean the input data of impulsive interference, jumps, and trends with time scales longer than the scale of the antenna beam in right ascension. When obtaining the mean flux densities for the entire observation time, we used only those recordings for which the noise dispersion at the location of the source was consistent with the noise properties of the total dataset; the method used to identify such recordings is described in [11].

We derived the mean flux density by applying optimal filtration to the average of the recordings, with the ith point for the filtration being the median of all the ith points for the cleaned input recordings. As a check, we also determined the mean flux density

$$\bar{S} = (\sum_{i}^{n} S_i)/n, \qquad (1)$$

where S_i is the flux density of the ith observation and n is the number of observations. There is no reason to introduce a weighting function here, since we are summing only those recordings that have already been determined to have noise characteristics consistent with those for the total dataset.

It is clear that the flux densities obtained in these two ways should be close and that substantial differences indicate the presence of a bad recording that has not been removed by the preliminary filtering. Our experience shows that significant differences are encountered only rarely, testifying to the correctness of the filtration algorithm applied. The few bad recordings that were still present are primarily those in which the antenna setup was incorrect. When significant flux-density differences were observed, we inspected all the corresponding recordings visually and removed any that appeared suspicious, then repeated the entire reduction procedure.

The measurement errors were also determined in two ways:

$$\sigma_\Sigma = \left(\sigma^2 / \sum_i A_i^2\right)^{\frac{1}{2}},$$

where σ^2 is the dispersion of the residual noise in the mean recordings after removing the detected source signal and A_i is the tabulated value of the antenna beam, and

$$\sigma_s = \left(\left(\sum_{i}^{n}(S_i - \bar{S})^2\right)\Big/ n(n-1)\right)^{\frac{1}{2}},$$

where $\bar{S}$ is the mean flux density derived using (1).

These two estimates should also be quite similar. If they corresponded to different distributions according to the Fisher criterion, we searched for bad recordings. In any case, we adopted the larger of the two estimates as the uncertainty in the measured flux density. In this approach, the resulting errors include the rms error in the flux density due to variability of the source during the series of observations.

3. RADIO AND OPTICAL COORDINATES

Table 1 presents the radio coordinates of the studied objects at epoch 2000.0 and the difference between the optical and radio coordinates for each object. We took the radio coordinates from the JVAS[1] catalog at 8.4 GHz [12] (rms coordinate error $0.014''$) and the NVSS[2] survey [13] at 1.4 GHz (average

[1] Jodrell Bank–VLA Astrometric Survey.
[2] NRAO VLA Sky Survey.

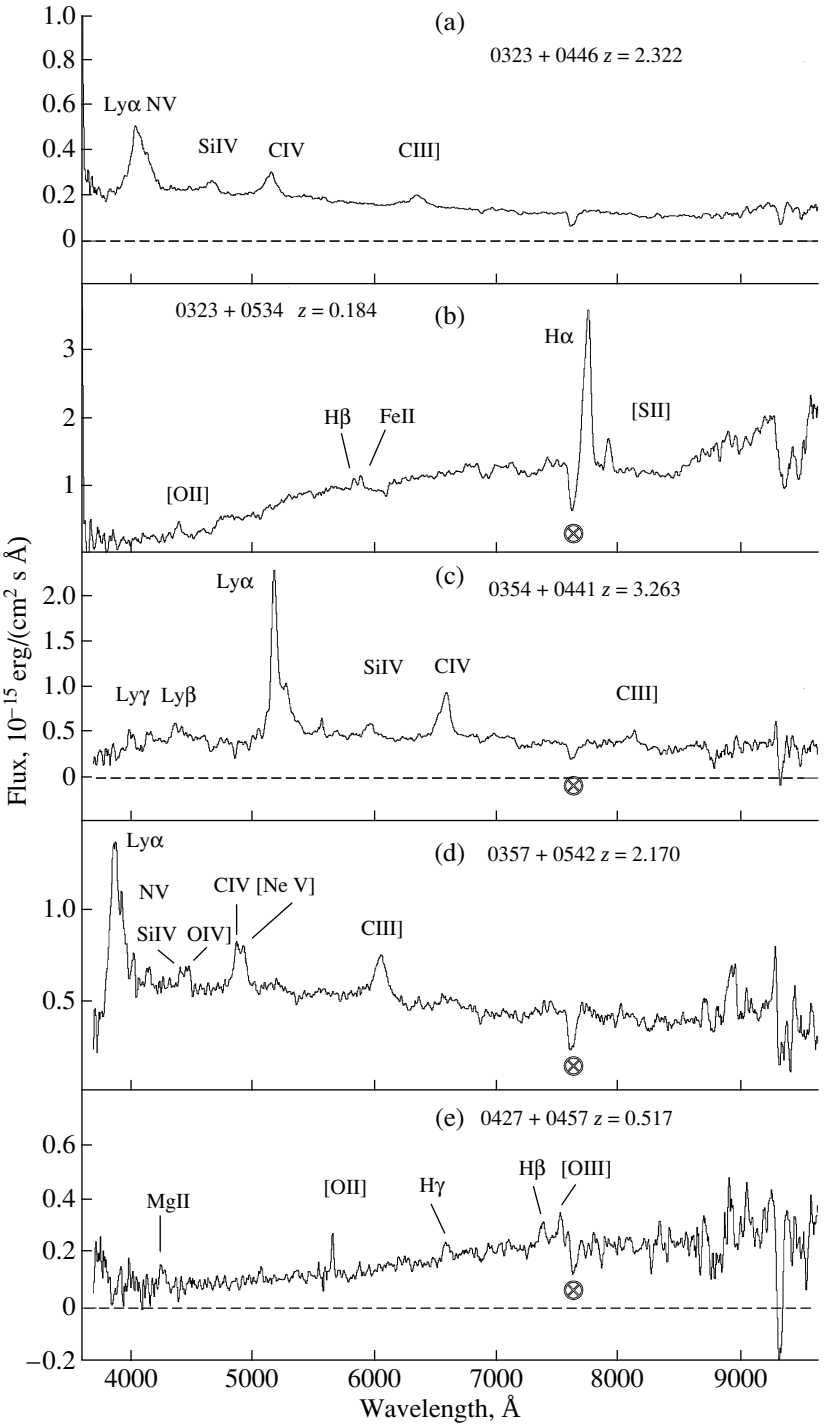

Fig. 1. Optical spectra of 0323+0446, 0323+0534, 0454+0441, 0357+0542, and 0427+0457 obtained on the 6-m telescope of the SAO.

rms errors about 0.11″ and 0.56″ in right ascension and declination, respectively). The source names are comprised of the hours and minutes of right ascension and degrees and minutes of declination corresponding to their coordinates. We obtained the optical coordinates from the USNO astrometric survey [14] or the Palomar Sky Survey APM database [15]. Taking into account the errors in both coordinates, the radio and optical coordinates for all the sources agree to within 3σ.

4. RESULTS

Figures 1–4 show optical and radio spectra of the objects.

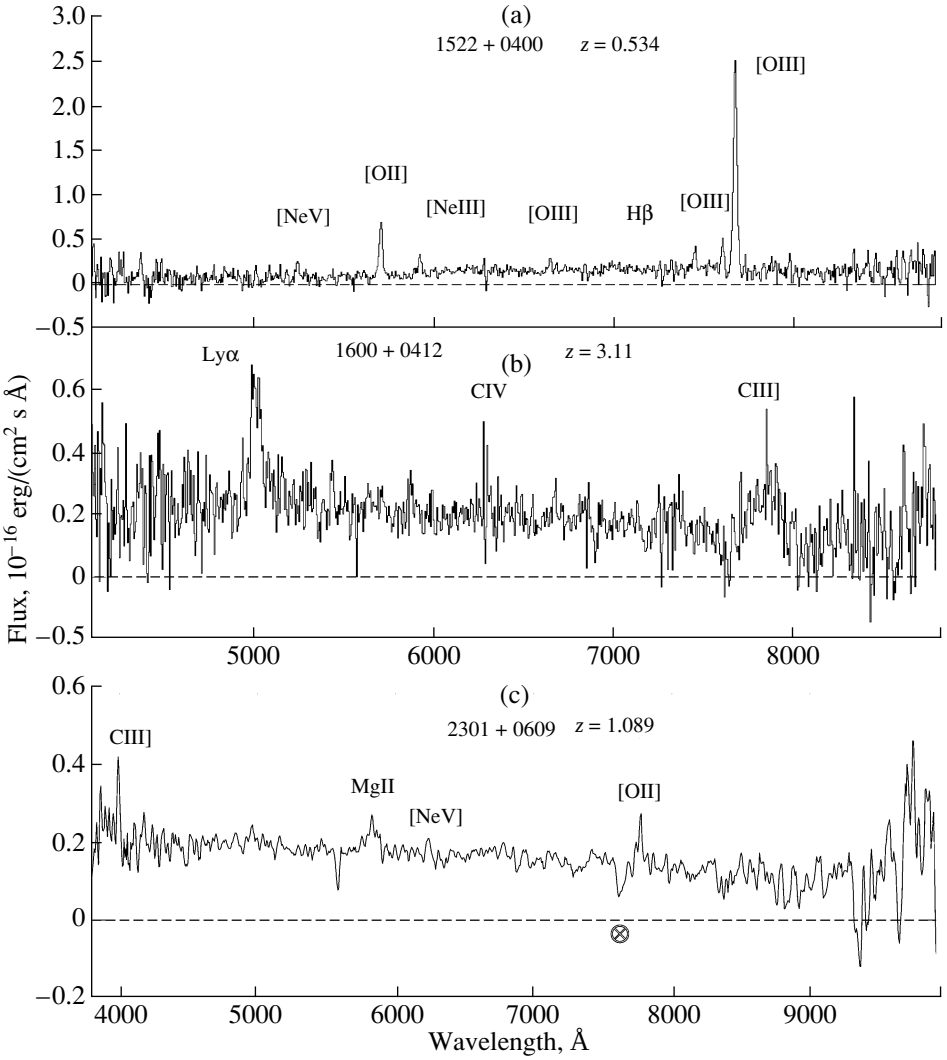

Fig. 2. Optical spectra of 1522+0400, 1600+0412, and 2301+0609 obtained on the 6-m telescope of the SAO.

Table 2 presents the optical data. The columns give (1) the source name, (2) lines present in the spectrum, (3) the rest-frame and observed wavelengths of these lines, (4) the corresponding redshift, (5) the classification of the object, (6) the observed B magnitude from [14, 15], (7) the observation date, and (8) the exposure in minutes.

Table 3 presents the flux densities of all the sources shown in Figs. 3 and 4. The columns give (1) the source name, (2)–(7) the flux densities and corresponding rms errors for 0.97, 2.3, 3.9, 7.7, 11.1, and 21.7 GHz in mJy, and (8) the observation epoch.

We present comments on individual sources below.

4.1. 0323+0446

The radio spectrum of this source, obtained in 1998 (Fig. 3a), falls off and then flattens toward higher frequencies. It can be approximated by the logarithmic parabola $\log S = -0.652 - 0.512 \log \nu + 0.171 \log^2 \nu$ (with the flux density in Jy and the frequency in GHz). The source does not display significant variability; over ten years of observations at 7.7 GHz obtained roughly once per year, the measured flux densities ranged from 135 ± 30 to 104 ± 4 mJy (covering a factor of 1.3 ± 0.3).

The optical spectrum had been obtained earlier at 4500–9000 Å using the 2.1-m telescope of the Guillermo Haro Observatory in Mexico. Based on the two lines CIV 1549 Å and CIII] 1909 Å, the object was classified as a quasar with a redshift of 2.322 [6]. Six lines can be identified in the optical spectrum obtained using the SAO 6-m telescope (Fig. 1a): a powerful, broad Lyα 1216 Å line (FWHM$\approx$ 130 Å), the NV 1240 Å line, the blended SiIV 1394,1403 Å doublet and OIV] 1406 Å line, and the CIV 1549 Å and

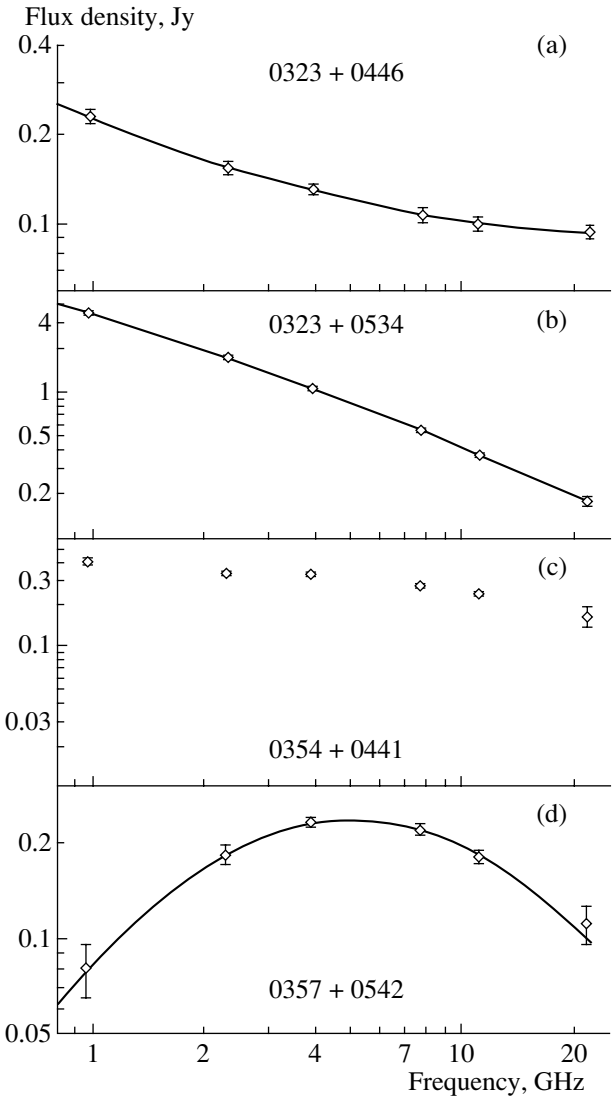

Fig. 3. Radio spectra of 0323+0446, 0323+0534, 0354+0441, and 0357+0542.

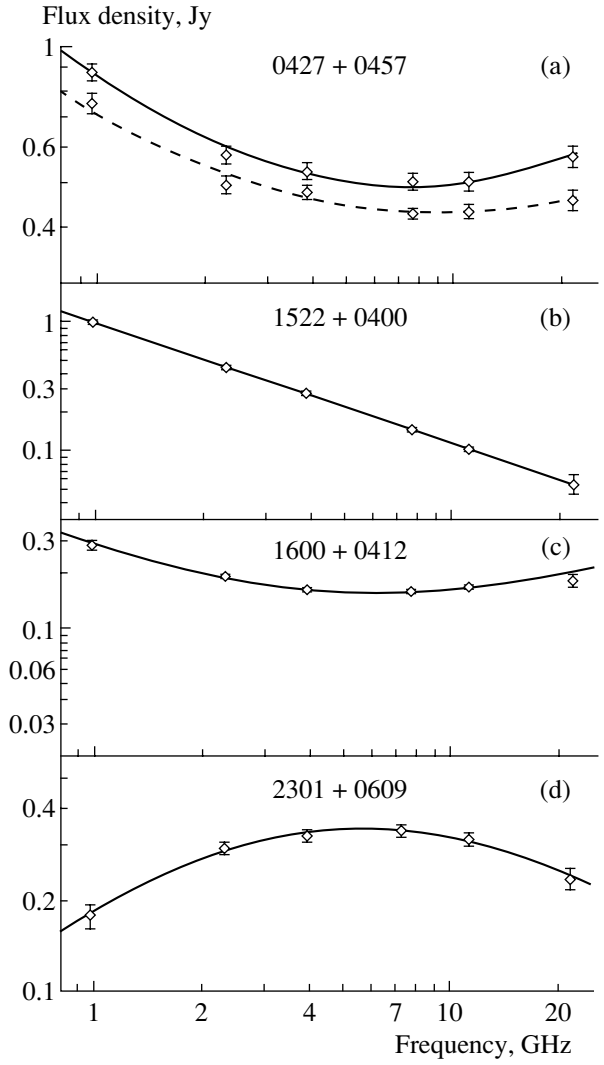

Fig. 4. Radio spectra of 0427+0457, 1522+0400, 1600+0412, and 2301+0609. The upper spectrum of 0427+0457 was obtained at epoch November 1997 and the lower at epoch July 1999.

CIII] 1909 Å lines. The redshift derived using all these lines is $z = 2.322 \pm 0.001$, confirming that the object is a quasar.

4.2. 0323+0534

The flux densities at 0.97–21.7 GHz are not variable, and the radio spectrum at 2.3–21.7 GHz is approximated well by the power law $S = 3976\,\nu^{-0.968}$ mJy (Fig. 3b). The spectrum flattens at lower frequencies. Based on the frequency of the turnover due to self-absorption ($\nu_m \approx 0.25$ GHz) and the flux density at this frequency ($S_m \approx 8$ Jy), we infer that the size of the radiating region exceeds 200 kpc (adopting the value H$= 10^{-4}$ Oe for the magnetic field in the jet).

Two Balmer lines—strong Hα 6563 Å and weak Hβ 4861 Å—can be identified in the optical spectrum (Fig. 1b), as well as the [OII] 3727 Å and FeII 4924 Å lines and the [SII] 6717, 6731 Å forbidden doublet. The widths of the hydrogen lines are FWHM$\approx$ 70 Å. All these lines are visible in emission, and the redshift is $z = 0.186 \pm 0.005$; the object is an emission-line radio galaxy.

4.3. 0354+0441

This source was observed in 1985 at 3.9 and 7.7 GHz. Figure 5a shows the flux-density variations at 7.7 GHz. Beginning in 1980, the flux density gradually decreased, reaching a minimum in 1995, after which it began to grow. The characteristic time

Table 2. Optical data

Source name	Lines present	Wavelength, Å	z	Spectral classification	B	Date	T, min
0323+0446	Lyα	1216/4040	2.322	QSO	19.1	Nov. 5, 2000	8
	SiIV/OIV]	1400/4650					
	CIV	1549/5145					
	CIII]	1909/6340					
0323+0534	[OII]	3727/4400	0.184	EmG	19.6	Nov. 4, 2000	10
	Hβ	4861/5820					
	FeII	4924/5890					
	Hα	6563/7760					
	[SII]	6724/7960					
0354+0441	Lyγ	973/4150	3.263	QSO	19.9	Nov. 4, 2000	10
	Lyβ	1026/4375					
	Lyα	1216/5185					
	NV	1240/5285					
	SiIV/OIV]	1400/5940					
	CIV	1549/6600					
	CIII]	1909/8135					
0357+0542	Lyα	1216/3865	2.170	QSO	19.6	Nov. 5, 2000	10
	NV	1240/3930					
	SiIV/OIV]	1400/4440					
	CIV	1549/4875					
	[NeV]	1575/4930					
	CIII]	1909/6056					
0427+0457	MgII	2798/4245	0.517	EmG	19.3	Nov. 5, 2000	10
	[OII]	3727/5654					
	Hγ	4340/6590					
	Hβ	4861/7375					
	[OIII]	4959/7522					
1522+0400	[NeV]	3426/5255	0.534	EmG	20.9	June 6, 2000	40
	[OII]	3727/5725					
	[NeIII]	3869/5930					
	[OIII]	4363/6655					
	Hβ	4861/7465					
	[OIII]	4959/7615					
	[OIII]	5007/7685					
1600+0412	Lyα	1216/5000	3.11	QSO	21.1	June 6, 2000	40
	CIV	1549/6320					
	CIII]	1909/7850					
2301+0609	CIII]	1909/4000	1.089	QSO	19.1	Nov. 2, 2000	10
	MgII	2798/5830					
	[NeV]	2973/6210					
	[OII]	3727/7780					

Table 3. Radio data

Source name	Flux densities and their errors, mJy						Epoch
	0.97 GHz	2.3 GHz	3.9 GHz	7.7 GHz	11.1 GHz	21.7 GHz	
0323+0446	230 21	149 06	132 05	105 06	97 05	95 06	01.1998
0323+0534	3568 52	1750 27	1070 10	556 06	380 07	190 12	07.1999
0354+0441	420 18	331 10	344 08	278 08	252 10	146 17	01.1998
0357+0542	80 15	182 11	232 09	220 07	181 06	112 15	07.1999
0427+0457	902 35	576 25	534 20	504 20	498 22	577 25	11.1997
	712 30	475 20	460 15	412 10	418 12	442 22	07.1999
1522+0400	1010 33	450 15	284 08	147 07	104 05	58 08	07.1999
1600+0412	289 15	189 07	159 05	163 06	172 07	182 16	01.1998
2301+0609	177 16	295 12	322 10	336 12	324 12	235 18	08.1997

scale for the variability (from maximum to minimum) is more than ten years. The 0.97–21.7 GHz spectrum in Fig. 3c was obtained in 1998 (diamonds). The spectrum is complex and cannot be approximated by a simple logarithmic parabola.

Three Lyman lines—Lyγ 973 Å, Lyβ 1026 Å, and powerful Lyα 1216 Å—can be identified in the optical spectrum (Fig. 1c), as well as the NV 1240 Å line, the blended SiIV 1394, 1403 Å doublet and OIV] 1406 Å line, and the CIV and CIII] 1549 and 1909 Å lines. The redshift derived using all the lines is $z = 3.263 \pm 0.002$, and we classified the object as a distant quasar.

4.4. 0357+0542

The 0.97–21.7 GHz spectrum of the source at epoch July 1999 can be well approximated with the logarithmic parabola $\log S = -1.076 + 1.266 \log \nu - 0.902 \log^2 \nu$; the spectral maximum is at 5.0 GHz, and the maximum flux density is 230 mJy (Fig. 3d). The source shows modest long-term variability. Observations at 7.7 GHz over 11 years obtained roughly once per year show flux-density variations from 275 ± 9 to 220 ± 5 mJy (covering a factor of 1.25 ± 0.05).

The optical spectrum (Fig. 1d) shows strong Lyα 1216 Å emission and the nearby NV line, the SiIV 1394, 1403 Å, doublet and the nearby OIV] 1406 Å line, the blended CIV 1549 Å and NeV 1575 Å lines, and the semiforbidden CIII] 1909 Å line at a redshift of $z = 2.17 \pm 0.007$. The object was classified as a quasar.

4.5. 0427+0457

This source displays appreciable long-term variability. Figure 5b shows the flux-density variations at 7.7 GHz from 1980 to 1999. The maximum 7.7-GHz flux-density variation has an amplitude $S_{\max}/S_{\min} = 2 \pm 0.14$. Figure 4a presents spectra obtained in November 1997 (upper) and July 1999 (lower). Both spectra have a minimum and can be approximated by the parabolas $\log S = -0.057 - 0.570 \log \nu + 0.327 \log^2 \nu$ and $\log S = -0.165 - 0.455 \log \nu + 0.236 \log^2 \nu$. Note the appreciable variability at low frequencies.

Five weak emission lines can be identified in the optical spectrum (Fig. 1d): MgII 2798 Å, the OII] 3727 Å forbidden line, the two Balmer lines Hγ 4340 Å and Hβ 4861 Å, and the [OIII] 4959 Å line at a redshift of $z = 0.517 \pm 0.008$. The object is an emission-line radio galaxy.

4.6. 1522+0400

The radio spectrum is power-law from 0.97–11.1 GHz, $S = 985\nu^{-0.927}$ mJy (Fig. 4b), and the flux density is not variable.

A strong [OIII] 5007 Å line, weaker OII] 3727 Å, [OIII] 4363 Å, and [OIII] 4959 Å lines, and weak NeV 3426 Å, [NeIII] 3869 Å, and Hβ 4861 Å lines can be identified in the optical spectrum (Fig. 2a). With the exception of Hβ, all these lines are forbidden and visible in emission. The redshift derived from all the lines is $z = 0.534 \pm 0.001$, and we classified the object as an emission-line radio galaxy.

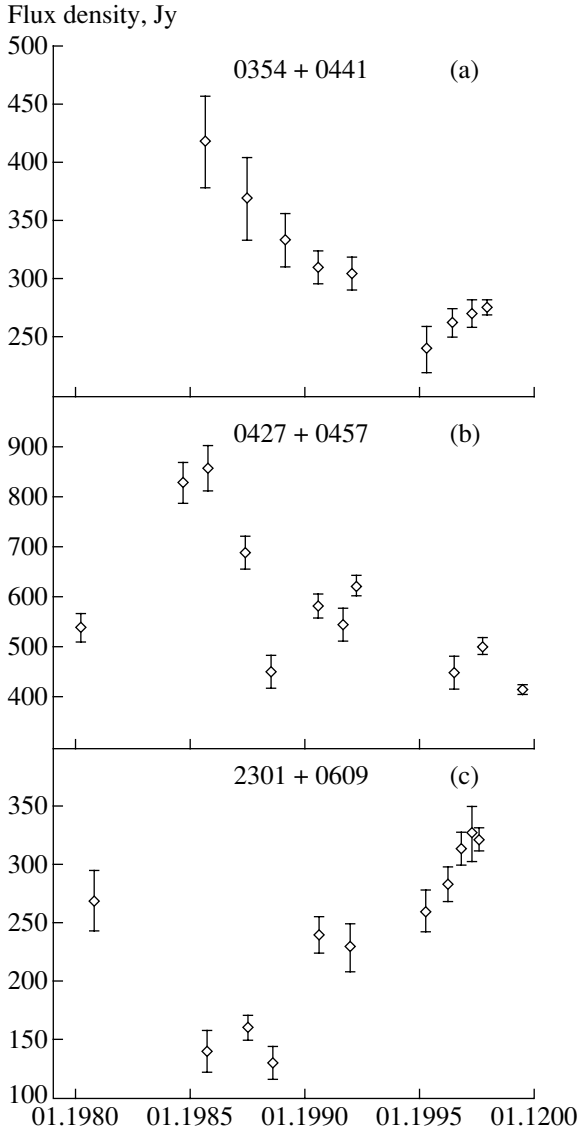

Fig. 5. 7.7-GHz light curves of 0427+0457 and 2301+0609. The flux densities before 1991 were obtained on the Southern sector and those after 1995 on the Northern sector of the RATAN-600 telescope.

4.7. 1600+0412

Observations made from 1989 through 1999 roughly once per year at 3.9 and 7.7 GHz did not reveal any flux-density variations within the errors. The ratio of the maximum and minimum flux densities measured at 7.7 GHz is $S_{\max}/S_{\min} = 1.1 \pm 0.15$. The spectrum (Fig. 4c) has a minimum near 6 GHz and can be approximated by the parabola $\log S = -0.553 - 0.617 \log \nu + 0.384 \log^2 \nu$ at epoch January 1998.

One broad line is clearly visible in the optical spectrum (Fig. 2b), which we have interpreted as a blend of Lyα 1216 Å and the nearby NV line at a redshift of $z = 3.11 \pm 0.01$. There are also weak CIV 1549 Å and HeII 1640 Å lines present near the noise level. We classified the object as a quasar.

4.8. 2301+0609

This source was observed at 3.9 and 7.5 GHz starting in 1980. Figure 5c presents the 7.7 GHz flux densities for 1980–1997. The flux density reached a minimum in 1987, after which it began to grow. The characteristic variability time scale (from maximum to minimum) is more than ten years, and the maximum flux-density variation at 7.7 GHz is $S_{\max}/S_{\min} = 2.7 \pm 0.5$. The spectrum (Fig. 4d) for August 1997 is well approximated by the logarithmic parabola $\log S = -0.733 + 0.695 \log \nu - 0.456 \log^2 \nu$, and has a maximum at 5.8 GHz, with the maximum flux density being 340 mJy.

Four emission lines can be identified in the optical spectrum (Fig. 2c): CIII] 1909 Å, MgII 2798 Å, and forbidden NeV 2973 Åand OII] 3727 Å. The redshift derived from these lines is $z = 1.089 \pm 0.003$, and the object was classified as a quasar.

5. CONCLUSIONS

Of the eight objects studied, five proved to be quasars (two with redshifts $z > 3$) and three to be emission-line radio galaxies. The radio galaxies 0323+0534 and 1522+0400 have constant flux densities and power-law spectra. The $z = 0.517$ emission-line radio galaxy 0427+0457 and $z = 1.089$ quasar 2301+0609 display appreciable radio variability. We did not detect any significant variability of the distant ($z = 3.11$) quasar 1600+0412 at 3.9 and 7.7 GHz over the ten years covered by our observations. As expected, long characteristic variability time scales are observed for all the objects with high redshifts. Nearly all the optical spectra show a rich selection of lines, enabling very accurate determinations of the corresponding redshifts.

6. ACKNOWLEDGMENTS

This work was supported by the Russian Foundation for Basic Research (project no. 01-02-16331), a Universities of Russia grant (project no. UR.02.03.005), and a grant of the State Science and Technology Program “Astronomy” (project no. 1.2.5.1).

REFERENCES

1. A. G. Gorshkov and V. K. Konnikova, Astron. Zh. **72**, 291 (1995) [Astron. Rep. **39**, 257 (1995)].
2. A. M. Botashov, A. G. Gorshkov, V. K. Konnikova, and M. G. Mingaliev, Astron. Zh. **76**, 723 (1999) [Astron. Rep. **43**, 631 (1999)].
3. A. G. Gorshkov, V. K. Konnikova, and M. G. Mingaliev, Astron. Zh. **77**, 407 (2000) [Astron. Rep. **44**, 353 (2000)].
4. V. Chavushyan, R. Mujica, A. G. Gorshkov, *et al.*, Pis'ma Astron. Zh. **26**, 403 (2000) [Astron. Lett. **26**, 339 (2000)].
5. V. Chavushyan, R. Mujica, A. G. Gorshkov, *et al.*, Astron. Zh. **78**, 99 (2001) [Astron. Rep. **45**, 79 (2001)].
6. V. Chavushyan, R. Mujica, R. Valdes, *et al.*, Astron. Zh. **79**, 771 (2002) [Astron. Rep. **46**, 697 (2002)].
7. A. B. Berlin, A. A. Maksyasheva, N. A. Nizhel'skiĭ, *et al.*, Abstracts of Papers, *XXVII Radio Astronomy Conference* (St. Petersburg, 1997), Vol. 3, p. 115 .
8. V. R. Amirkhanyan, A. G. Gorshkov, and V. K. Konnikova, Astron. Zh. **69**, 225 (1992) [Sov. Astron. **36**, 115 (1992)].
9. N. S. Soboleva, A. V. Temirova, and T. V. Pyatunina, Preprint SAO (Spets. Astrofiz. Obs., Nizhniĭ Arkhyz, 1986), p. 32.
10. A. G. Gorshkov and O. I. Khromov, Astrofiz. Issled. (Izv. Spets. Astrofiz. Obs.) **14**, 15 (1981).
11. A. G. Gorshkov and V. K. Konnikova, Astron. Zh. **73**, 351 (1996) [Astron. Rep. **40**, 314 (1996)].
12. I. W. A. Browne, Mon. Not. R. Astron. Soc. **293**, 257 (1998).
13. J. J. Condon, W. D. Cotton, E. W. Greisen, *et al.*, Astron. J. **115**, 1693 (1998).
14. D. Monet, A. Bird, B. Canzian, *et al.*, *USNO-SA 1.0* (U.S. Naval Observatory, Washington, 1996).
15. R. L. Pennington, R. M. Humphreys, S. C. Odewahn, *et al.*, Pub. Astron. Soc. Pac. **105**, 103 (1993).

Translated by D. Gabuzda